ADVANCED HEALTHCARE MATERIALS
www.advhealthmat.de

Bioinspired Liposomes for Oral Delivery of Colistin to Combat Intracellular Infections by *Salmonella enterica*

Sara Menina, Janina Eisenbeis, Mohamed Ashraf M. Kamal, Marcus Koch, Markus Bischoff, Sarah Gordon, Brigitta Loretz, and Claus-Michael Lehr**

Bacterial invasion into eukaryotic cells and the establishment of intracellular infection has proven to be an effective means of resisting antibiotic action, as anti-infective agents commonly exhibit a poor permeability across the host cell membrane. Encapsulation of anti-infectives into nanoscaled delivery systems, such as liposomes, is shown to result in an enhancement of intracellular delivery. The aim of the current work is, therefore, to formulate colistin, a poorly permeable anti-infective, into liposomes suitable for oral delivery, and to functionalize these carriers with a bacteria-derived invasive moiety to enhance their intracellular delivery. Different combinations of phospholipids and cholesterol are explored to optimize liposomal drug encapsulation and stability in biorelevant media. These liposomes are then surface-functionalized with extracellular adherence protein (Eap), derived from *Staphylococcus aureus*. Treatment of HEp-2 and Caco-2 cells infected with *Salmonella enterica* using colistin-containing, Eap-functionalized liposomes resulted in a significant reduction of intracellular bacteria, in comparison to treatment with nonfunctionalized liposomes as well as colistin alone. This indicates that such bio-invasive carriers are able to facilitate intracellular delivery of colistin, as necessary for intracellular anti-infective activity. The developed Eap-functionalized liposomes, therefore, present a promising strategy for improving the therapy of intracellular infections.

1. Introduction

Combating intracellular pathogens remains a considerable challenge, due to the ability of these infectious organisms to invade mammalian cells and even more take refuge in intracellular vacuoles. This problem is compounded by the poor permeability of some anti-infectives, which limits their use against such pathogens.[1] According to the WHO report, *Salmonella* is one such challenging intracellular pathogen, affecting 11 to 21 million people every year, and 128 000 to 161 000 deaths occur annually worldwide (WHO Report, Immunization, Vaccines and Biologicals, 11 September 2018). Fluoroquinolones and third generation cephalosporins are commonly used as first line therapy for *Salmonella* infections; however, due to a significant increase in antimicrobial resistance[2,3] combined with recent reports of toxic and metabolic side effects resulting from the use of fluoroquinolones[4] (FDA Report, Drug Safety and Availability, 7 October 2018), there is an urgent need for alternative treatment options. One such option is the polypeptide antibacterial agent colistin, which was commonly employed in the 1950s for its potent activity against multidrug resistant (MDR) pathogens.[5] The use of colistin was abandoned due to its high level of neurotoxicity and nephrotoxicity, however the desperate need for new therapies has seen it re-emerge as a "last resort" treatment option for Gram-negative MDR infections.[6,7] Its use is currently restricted to parenteral administration due to a low oral absorption and bioavailability, leading to considerable research interest in optimization of oral drug activity with minimization of toxic effects.[8–11]

The emergence of nanotechnology-based medicines in recent years has proven to be an effective strategy for the treatment of infectious diseases.[12] The encapsulation of anti-infectives into nanocarrier systems may afford targeted delivery to the site of infection, by overcoming permeability limitations across

S. Menina, M. A. M. Kamal, Dr. S. Gordon, Dr. B. Loretz, Prof. C.-M. Lehr
Helmholtz Institute for Pharmaceutical Research Saarland (HIPS)
Helmholtz Center for Infection Research (HZI)
Saarbrücken 66123, Germany
E-mail: Brigitta.Loretz@helmholtz-hips.de;
Claus-Michael.Lehr@helmholtz-hips.de

The ORCID identification number(s) for the author(s) of this article can be found under https://doi.org/10.1002/adhm.201900564.

DOI: 10.1002/adhm.201900564

S. Menina, Prof. C.-M. Lehr
Department of Pharmacy
Saarland University
Saarbrücken 66123, Germany
J. Eisenbeis, Prof. M. Bischoff
Institute of Medical Microbiology and Hygiene
Saarland University
Homburg 66421, Germany
Dr. M. Koch
Institute for New Materials
Saarland University
Saarbrücken 66123, Germany
Dr. S. Gordon
School of Pharmacy and Biomolecular Sciences
John Moores University
Liverpool L3 3AF, UK

cellular barriers and at the same time avoiding adverse off-target effects.[13,14] Encapsulating colistin into such a delivery system could therefore offer the possibility to administer a lower dose while still maintaining its antibacterial efficacy, and thereby minimize its systemic toxicity.[15] In addition, such a system would offer the opportunity to administer colistin orally, by protecting colistin from the harsh conditions of the gastrointestinal (GI) tract.[16] Nevertheless, only few studies have investigated the ability of colistin-loaded nanocarriers to be administered by alternative, noninjectable routes, with the main focus to date being on the treatment of pulmonary infections by inhalation/pulmonary administration.[17–19] Liposomes are one of the most commonly utilized nanocarriers for the intracellular delivery of anti-infectives, providing the potential for improved cell penetration and reduced anti-infective-associated toxicity.[13,20,21] The use of liposomes for oral administration faces many challenges, including the low pH of the stomach and the presence of digestive enzymes, which may disrupt liposomal lipid bilayers and result in drug leakage.[22] Recent efforts have indicated the ability to formulate GI-stable liposomes by manipulating lipid compositions or employing surface coatings; however, this is an area of ongoing research need.[23–25] The potential, further enhancement of the ability of nanoparticulate delivery systems to access and treat intracellular infections by functionalization of their surfaces with invasive moieties is also an area that warrants further investigation.[26] For instance, several strategies have been utilized to target and treat infected phagocytic cells. Mannose-conjugated nanogel could assist in antibiotic delivery into phagocytic cells via the mannose-receptors in macrophages.[27] In another study, extracellular vesicles of *S. aureus* were used to coat vancomycin-loaded nanoparticles to target infected macrophages.[28] In the case of nonphagocytic cells, liposomes functionalized with invasin (InvA497), a membrane protein responsible for the invasive ability of *Yersinia* species of bacteria such as *Y. pseudotuberculosis*, have been shown to significantly improve the intracellular delivery of the poorly permeable antibiotic gentamicin into epithelial cells.[29] This strategy was adopted in order to mimic the pathway by which *Y. pseudotuberculosis* invades eukaryotic cells, through the interaction of bacterial InvA497 with cellular $\alpha_5\beta_1$ integrin receptors.[30] Many other bacteria possess a similar invasive strategy, for instance, *Staphylococcus aureus* possesses proteins that mediate its invasion into and ability to shelter within mammalian cells, such as fibrinogen binding protein (FnBP) and extracellular adherence protein (Eap). Eap is a secreted protein composed of composed of 4 to 6 EAP domains (≈97 amino acid residue domains that share homology with the C-terminal domain of bacterial superantigens) joined by 9–11 amino acid residue linker regions, yielding in proteins with a total mass of about 50 to 70 kDa (depending on the *S. aureus* strain), joined by unknown 9–12 residue linker regions.[31] This excreted protein is able to bind to a number of host cell extracellular matrix components and to rebind to the surface of *S. aureus*, and thereby promotes the invasion of *S. aureus* into cells.[32] This secretion and rebinding mechanism is similar to internalin (InlB) from *Listeria monocytogenes*, which can be associated with the bacteria but is also found in the supernatant in free form.[33] Moreover, it has been shown that mixing Eap with noninvasive bacteria or fluorescent beads promotes their internalization into eukaryotic cells.[34,35] Interestingly, despite its well-documented ability to promote effective intracellular invasion of *S. aureus* and other bacteria, the exact mechanism by which Eap mediates bacterial internalization remains unclear;[36] to date, it has also not been investigated as a means for promoting intracellular delivery of antibiotic-containing carrier systems. In the current work therefore, various liposomal formulations loaded with colistin were first investigated for their potential to act as oral delivery systems, by optimizing their stability in various biorelevant media. The most stable liposomes were then surface-functionalized with Eap, and further characterized. The efficiency of colistin-loaded, Eap-functionalized liposomes to deliver colistin into epithelial cells was finally investigated, using HEp-2 and Caco-2 epithelial cells infected with the enteroinvasive bacterium *Salmonella enterica*.

2. Results and Discussion

2.1. Preparation and Characterization of Colistin-Loaded Liposomes

In order to prepare liposomes with the ability to withstand the harsh conditions of the gastrointestinal tract, saturated long carbon chain phospholipids were used.[37] In addition, 30 mol% of cholesterol was utilized, which has been shown to increase the integrity of vesicles by promoting alignment of phospholipids alkyl chains, enabling a condensed packing of the lipid bilayer.[38,39] This results in either shifting or elimination of the phase transition of liposomes inducing more orderly behavior of lipid fatty acid chains.[39,40] Three different liposomal formulations consisting of 1,2-dipalmitoyl phosphatidylcholine/1,2-dipalmitoyl-sn-glycero-3-phospho-ethanolamine-*N*-(Glutaryl)/cholesterol (DPPC/DPPE-GA/CHOL), 1,2-distearoyl-sn-glycero-3-phosphocholine/DPPE-GA/cholesterol (DSPC/DPPE-GA/CHOL), and DPPC/DSPC/DPPE-GA /CHOL were prepared, loaded with various colistin concentrations (1, 2, 3, 4, 5, and 10 mg mL^{-1}), and characterized (Col-Lip-1, Col-Lip-2, and Col-Lip-3 respectively). The size of all liposome formulations was ≈200 nm, with all formulations having a low polydispersity index and a negative surface charge (Figure S1a–c, Supporting Information). Colistin was encapsulated with entrapment efficiencies (EE) ranging from 10% to 60%, inversely proportional with colistin concentration (Figure S1d, Supporting Information), while loading capacities (LC) ranged from 20% to 80%, proportional to colistin concentrations (Figure S1e, Supporting Information). This phenomenon can be explained by the ability of colistin to disturb liposomal formulations, as a result of its positively charged nature; thus, an increase in colistin concentration may lead to progressive disruption of the liposomal structure and a reduced capacity for drug incorporation. In contrast, the proportional increase in LC may be explained by a progressive decrease in liposome yield with increasing colistin concentration. A similar effect was observed by Wallace et al. using lipid film hydration method as well as freeze drying technique.[41] The effect of colistin on artificial membrane models has also been investigated previously and has shown various effects ranging from increasing surface roughness to pore formation and leakage of contents.[42] Liposomes prepared using 4 mg mL-1 of colistin with ≈30% EE and 50% LC were employed for further studies since the EE and LC variations were minor between the three formulations. Scanning (SEM) and Cryo-transmission (Cryo-TEM)

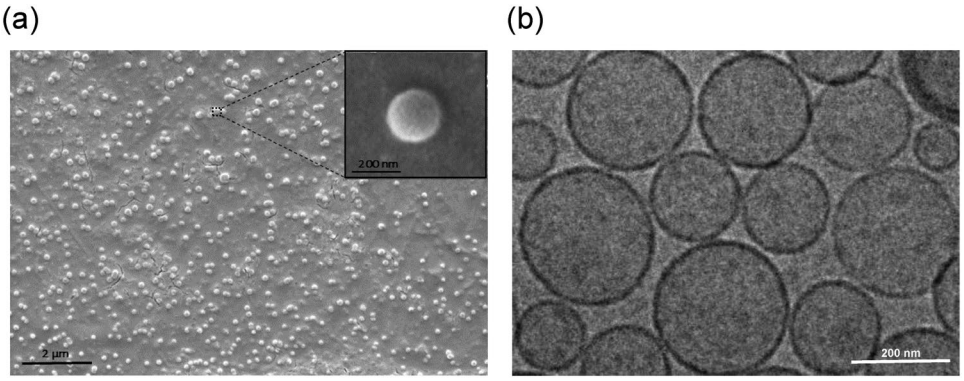

Figure 1. Representative images of Col-Lip-1 using a) scanning electron microscopy and b) Cryo-Transmission electron microscopy, showing unilamellar spherical shaped liposomes of 200 nm.

electron microscopy images of Col-Lip-1 containing 4 mg mL-1 colistin (as a representative formulation) confirmed the presence of spherical particles of ≈200 nm in diameter, in line with the dynamic light scattering (DLS) results of Figure S1 in the Supporting Information (**Figure 1**). However, further optimization of the formulation process was carried out including an increase of rotation speed during the lipid film hydration step, as well as the employment of a sonication step before liposome extrusion (Experimental Section), that yielded an increase of EE to over 55% and gave LC results of 50% (**Table 1**). Encapsulation of hydrophilic drugs into liposomes using lipid film hydration has been associated with low EE compared to other methods.[43,44] Wallace et al. have achieved 40% EE of colistin in 1,2-dioleoyl-sn-glycero-3-phosphocholine-based liposomes prepared with lipid hydration using 5 mg mL^{-1} of colistin.[41] The EE obtained in this work, therefore, are comparable to the previous studies and considered reasonably high using such a method, which could be attributed potentially to the ability of colistin to incorporate into the lipid bilayer.[41,45]

Colistin-loaded liposomes were subjected to thermal characterization using differential scanning calorimetry (DSC)[46] (Figure S2, Supporting Information). Incorporation of 30% cholesterol into the liposomes resulted in an abolishment of the phase transition of DPPC (41 °C) and DSPC (55 °C) in the determined range of 0 to 80 °C.[47,48] The loading of colistin into the liposomes did not affect the lipid bilayers in comparison to drug-free liposomes (data not shown).

2.2. Stability in Biorelevant Media

The prepared liposomal formulations are proposed as delivery systems to be used for oral administration. Therefore, those liposomes should withstand the harsh conditions of the gastrointestinal tract and thereby retain their encapsulated colistin, preventing its burst release and degradation. To assess the stability of liposomes within conditions characteristic of the environment within the gastrointestinal tract, various biorelevant media were employed. Fasted state simulated gastric fluid (FaSSGF) was used as a medium mimicking the composition of fluids in a fasted stomach. This medium is mainly characterized by a low pH (1.6) and presence of pepsin (0.1 mg mL^{-1}), which is one of the main digestive enzymes in the GI tract.[49] Fasted state simulated intestinal fluid without enzymes (FaSSIF) or with enzymes (FaSSIF-Enz) were employed, as established media mimicking the composition of fluids in the upper small intestine in the absence of food[50,51] Moreover, to simulate the conditions in the small intestine after meal intake, fed state simulated intestinal fluid (FeSSIF) was used.[52] Liposomes were incubated within each medium at 37 °C for 5 h, which is the estimated total time required for an orally administrated drug to be absorbed.[53] The amount of released colistin as well as its integrity were monitored hourly via high-performance liquid chromatography (HPLC), and the colloidal parameters of liposomes were also measured.

Col-Lip-1 showed a burst release of colistin of ≈10% to 15% upon addition to FaSSGF, FaSSIF, and FaSSIF-Enz, following which less than 20% of colistin was observed to be released for the remainder of the 5 h incubation period. Incubation of Col-Lip-1 in PBS (control medium) did not show any release of colistin during the 5 h study period, while 58% of colistin was released from Col-Lip-1 incubated in FeSSIF (**Figure 2**a). Col-Lip-2 released less than 10% of total drug load in PBS, FaSSGF and FaSSIF, whereas 32% and 18% of colistin was released in FaSSIF-Enz and FeSSIF respectively over a 5 h period (Figure 2b). In contrast, Col-Lip-3 showed a release of 5% in FaSSIF and a maximum of 20% in other media after the 5 h (Figure 2c). The considerable release of colistin from Col-Lip-1 in FeSSIF indicates a vulnerability of these liposomes

Table 1. Characteristics of liposomes loaded with 4 mg mL^{-1} colistin.

	Formulation	Molar ratio	Size [nm]	PDI	ζ-Potential [mV]	EE [%]	LC [%]
Col-Lip-1	DPPC:DPPE-GA:CHOL	1:0.2:1	211.8 ± 1.7	0.05 ± 0.1	−21.0 ± 0.6	55.3 ± 5.2	49.8 ± 0.4
Col-Lip-2	DSPC:DPPE-GA:CHOL	1:0.2:1	201.3 ± 1.0	0.05 ± 0.1	−17.3 ± 0.3	61.7 ± 5.7	50.9 ± 0.7
Col-Lip-3	DPPC:DSPC:DPPE-GA:CHOL	1:1:0.2:1	202.7 ± 1.4	0.03 ± 0.1	−15.3 ± 1.2	59.3 ± 4.3	50.4 ± 0.3

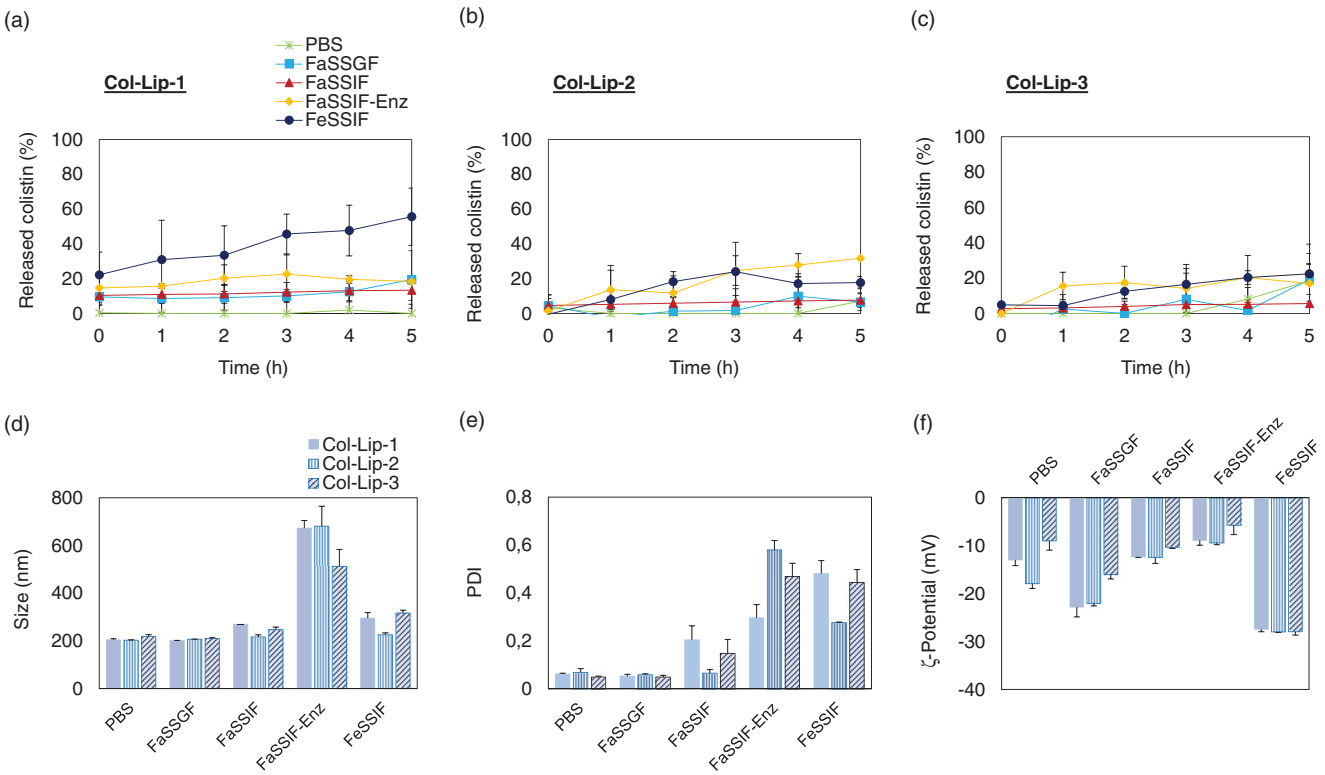

Figure 2. Cumulative percentage of colistin released from liposomes a) Col-Lip-1, b) Col-Lip-2 and c) Col-Lip-3 in different biorelevant media: FaSSGF (square), FaSSIF (triangle), FaSSIF-Enz (diamond), FeSSIF (circle), and PBS (star) over 5 h. Stability study results d) size e) PDI and f) ζ-Potential of liposomal formulations Col-Lip-1, Col-Lip-2, and Col-Lip-3 after 5 h incubation in biorelevant media. Data are shown as mean ± SEM from three independent replicates ($N = 3$, $n = 9$).

to high concentrations of bile salts and the presence of lipolysis products, and therefore an inability to effectively retain colistin within the fed small intestine. Col-Lip-2 and Col-Lip-3 showed a better stability in the GI-simulated media, which could be attributed to the presence of the longer chain phospholipid DSPC in their lipid bilayers. These findings are in line with what has been reported previously, namely, that DSPC-containing liposomes are able to withstand the potentially destabilizing effects of bile salts and enzymes.[54,55] With respect to the colloidal parameters, no notable changes were observed in liposomal size and polydispersity index (PDI) in all tested media for the three formulations, except in FaSSIF-Enz, where the size increased to more than 600 nm and PDI to more than 0.4 (Figure 2d,e). However, in this particular case, the presence of protein (pancreatin) in the medium is likely to have interfered with the DLS measurements, as it has been demonstrated that the formation of protein–protein or protein–liposome aggregates (as well as protein corona) can significantly affect DLS results.[56] Thus, Cryo-TEM was employed for further investigation. Imaging of stability study samples in FaSSIF-Enz (liposomes diluted 1:10 in the medium) showed the presence of aggregates as well as intact spherical liposomes of ≈200 nm in diameter (Figure S3, Supporting Information). In FeSSIF, the PDI increased in the three formulations despite the unchanged average size. This is due to the presence of bile salts and lipid micelles in this medium, which could be measured by DLS (≈70 nm). Other studies employing biorelevant media simulating human intestinal fluids have similarly demonstrated the presence of various colloidal assemblies in these media, ranging from ellipsoidal micelles to larger structures including vesicles, rods, and discs.[57–62] The ζ-potential of all liposomal formulations was negative in all tested media; the magnitude of surface charge varied from ≈−6 to −30 mV however, reflective of the different media compositions and their subsequent effects on liposome surface charge.[63] Further experiments were carried out using only Col-Lip-2 and Col-Lip-3 formulations, as these were more stable in terms of chemical and colloidal parameters in comparison to Col-Lip-1.

2.3. Functionalization of Colistin-Loaded Liposomes with Eap

In order to enhance the internalization of liposomes into epithelial cells, the bacteria-derived invasion protein Eap was investigated for its ability to promote liposome cellular uptake. Liposomes were functionalized with 40 μg mL^{-1} Eap either by covalent coupling, using 4-(4,6-dimethoxy-1,3,5-triazin-2-yl)-4-methylmorpholinium (DMTMM) as a cross-linker, or by physical adsorption to liposomal surfaces. The quantification of Eap associated with liposomal surfaces could not be performed by commonly used methods such as bicinchoninic acid or Bradford assays due to the interference of colistin, and therefore sodium dodecyl sulfate polyacrylamide gel electrophoresis

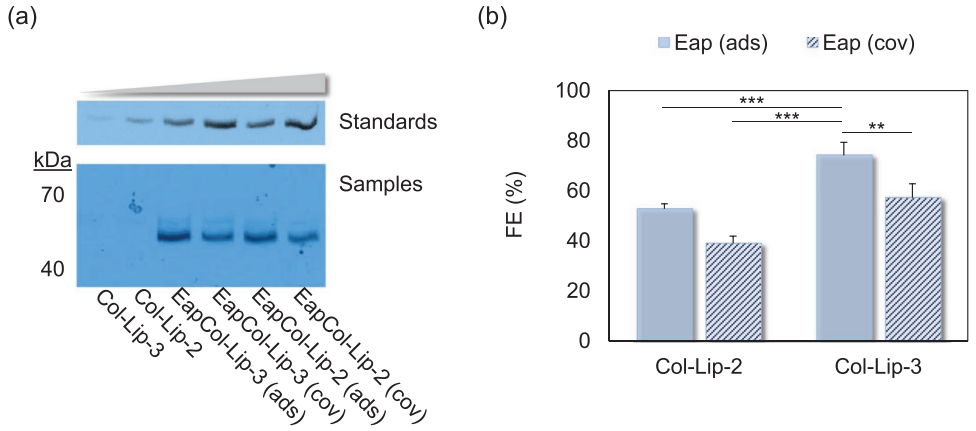

Figure 3. a) SDS-PAGE gel of Eap standards (5, 10, 20, 30, 40, and 50 μg mL^{-1}) as well as non-functionalized colistin liposomes (Col-Lip-2 and Col-Lip-3), Eap-functionalized colistin liposomes via surface adsorption (EapCol-Lip-2 (ads) and EapCol-Lip-3 (ads)) or via covalent coupling (EapCol-Lip-2 (cov) and EapCol-Lip-3 (cov)). b) Functionalization efficiency of liposomes functionalized with Eap via surface adsorption ('Eap (ads)', solid bars) and covalent coupling ('Eap (cov)', striped bars). Data are shown as mean ± SEM from three independent replicates ($N = 3$, $n = 9$). Significance was defined as $^{**}P < 0.01$ and $^{***}P < 0.001$.

(SDS-PAGE) was used to quantify the functionalization efficiency (FE). SDS-PAGE gels showed a distinct Eap band at 55 kDa in both functionalized liposome samples and standards (**Figure 3**a). The efficiency of Eap functionalization of Col-Lip-3 was significantly highly than that of Col-Lip-2, utilizing both physical adsorption (75% and 52% respectively) and covalent coupling methods (57% and 38% respectively) (Figure 3b). The high FE achieved by physical adsorption could be attributed to the considerable adhesive properties of Eap, via electrostatic interactions.[64] For further experiments, Col-Lip-3 functionalized with Eap via physical adsorption was employed, due to the high FE obtained in this case.

2.4. Uptake of Eap-Functionalized Liposomes in Epithelial Cells

Uptake studies were performed by addition of rhodamine-labeled liposomes (red fluorescence) to two different epithelial cell lines: Caco-2 cells and HEp-2 cells. The percentage of fluorescent cells (indicative of cells containing liposomes) was then determined using flow cytometry (FACS). Caco-2 cells were grown as a confluent monolayer until transepithelial electrical resistance (TEER) values reached >500 Ω cm^2 (Figure S4, Supporting Information) to resemble the barrier properties of the small intestinal epithelial layer.[65,66] Eap and colistin as well as liposomal lipid concentrations used in this study were not cytotoxic for either cell type (Figure S5, Supporting Information). Different concentrations of bound Eap (5, 10, and 20 μg mL^{-1}) were applied on HEp-2 cells (1 and 2 h incubation) and Caco-2 monolayers (2 and 4 h incubation). Uptake results showed that only 3% of nonfunctionalized Col-Lip-3 were taken up by HEp-2 cells (**Figure 4**a), whereas 20% of Caco-2 cells were positively labeled after 2 h (Figure 4c). This may point to a difference in HEp-2 and Caco-2 cell mechanisms of particle uptake, further addressed below. Upon the incubation of HEp-2 cells with Eap-functionalized liposomes, the percentage of positively labeled cells increased in a time- and concentration-dependent manner, reaching almost 100% using 10 and 20 μg mL^{-1}of Eap after 2 h (Figure 4a,b). For Caco-2 cell monolayers, a 2 h incubation with liposomes functionalized with 20 μg mL^{-1} of Eap resulted in 75% of cells being fluorescently labeled (45% when 10 μg mL^{-1} Eap was employed for functionalization, and 12% with 5 μg mL^{-1} Eap) (Figure 4c). Therefore, cells were further incubated for 4 h with Eap-functionalized liposomes, which resulted in a significant increase in uptake, reaching almost 100% when 20 μg mL^{-1} Eap was used for functionalization (Figure 4c,d).

In another approach to study the uptake of Eap-functionalized liposomes, cells were incubated (HEp-2 cells: 2 h, Caco-2 cells: 4 h) with liposomes, stained, and visualized using confocal microscopy. The two cell lines were incubated with liposomes for different incubation periods in order to reflect the time period required for optimal uptake, as seen in Figure 4. Similarly to the flow cytometry-based uptake results, only liposomes which had been functionalized with Eap were seen to be internalized into HEp-2 cells (visible as red cytosolic staining in **Figure 5**a, and Figures S6a, and S7a in Supporting Information). With respect to Caco-2 cells, Eap-functionalized liposomes were present in almost all visualized cells; however, nonfunctionalized liposomes could also be detected within a small number of cells (Figure 5b, and Figures S6b and S7b in Supporting Information). This observation also fits with the results obtained from flow cytometry analysis, indicating that, in contrast to HEp-2 cells (Figure 5a), Caco-2 cells are able to take up nonfunctionalized liposomes to a certain degree (Figure 5b).

In order to investigate this further, and to also probe the existence of any difference in the mechanism of uptake of Eap-functionalized liposomes, an uptake assay at 4 °C was performed with both cell types. At this temperature, Caco-2 cells showed a significant decrease in the percentage of rhodamine-labeled cells (14%) compared to the uptake at 37 °C. Interestingly, their uptake by HEp-2 cells was not affected at this temperature (**Figure 6**a,b). The temperature dependency of Caco-2 cells uptake points toward an energy-dependent mechanism, which has been previously reported using different types

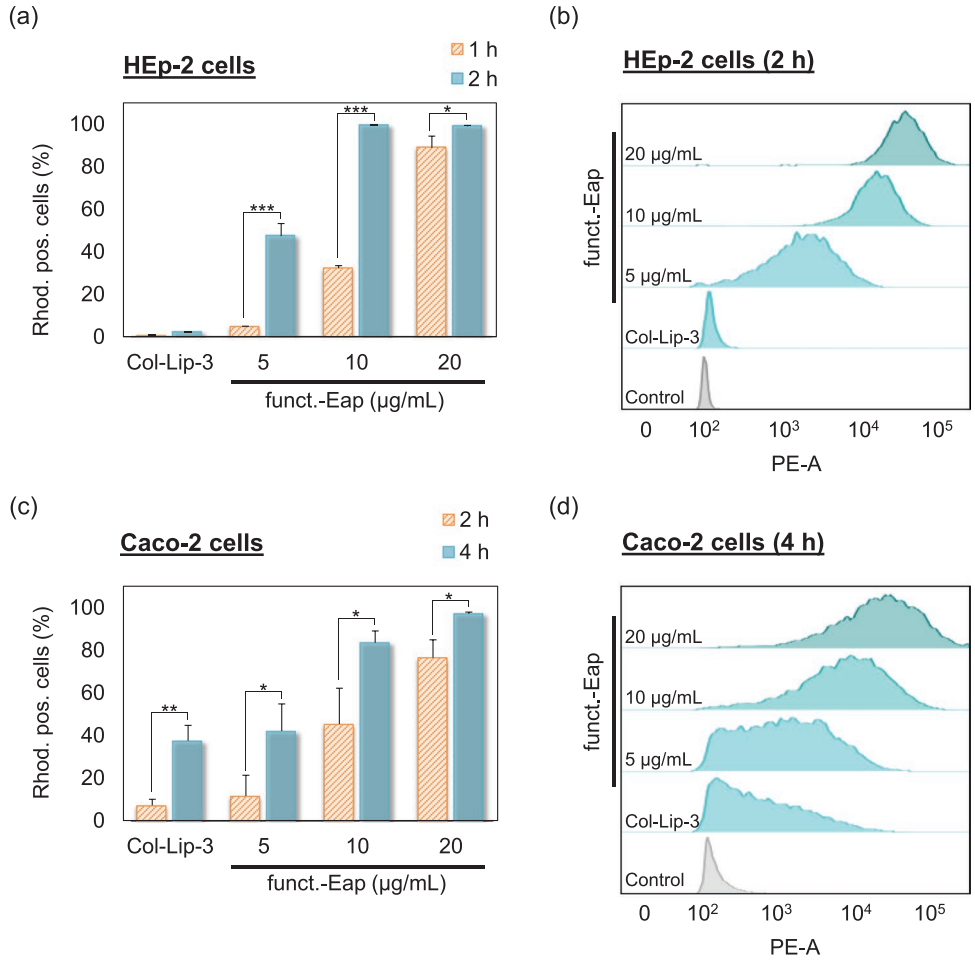

Figure 4. a) Percentages of rhodamine-positive HEp-2 cells (1 and 2 h) and b) the corresponding histogram plots, c) percentages of rhodamine-positive Caco-2 cells (2 and 4 h) and d) the corresponding histogram plots resulting from treatment of cells with non-functionalized liposomes (Col-Lip-3) and Col-Lip-3 functionalized with different Eap concentrations (5, 10 and 20 μg mL^{-1}). Controls were the untreated cells. Data are shown as mean ± SEM from three independent replicates ($N = 3$, $n = 9$). Significance was defined as $^{*}P < 0.05$, $^{**}P < 0.01$ and $^{***}P < 0.001$.

of liposomes.[67,68] However, the uptake mechanism of Eap as mentioned earlier, is not yet well understood and more studies are needed to characterize the specific pathways involved in the binding and internalization of this protein.[36,69] Therefore, an uptake experiment in Caco-2 cells was conducted using endocytosis inhibitors (Figure 6c). Results showed a decrease of the uptake percentage of ≈8% after using Cytochalasin D as an inhibitor of actin polymerization and, therefore, inhibition of macropinocytosis.[70,71] Moreover, a decrease in uptake of ≈17% was observed when using either chlorpromazine as an inhibitor of clathrin-dependent endocytosis (which translocates clathrin from the cell surface to the intracellular compartment),[72,73] or MβCD + lovastatin as an inhibitor of clathrin-independent (and caveolae-independent) endocytosis mechanisms.[74] In addition, 40% of the uptake was inhibited in the presence of the caveolae-dependent endocytosis inhibitor "filipin III," which acts as a sterol-binding agent that disrupts caveolae and caveolae-like structures.[75,76] These results show that the internalization of Eap-functionalized liposomes by Caco-2 cells involves pathways which predominantly utilize caveolae-mediated endocytosis.

2.5. Impact of Eap-Functionalized Liposomes Containing Colistin on Infected Cells

Conventional liposomes typically composed of only phospholipids and/or cholesterol carrying antibacterial agents have previously been shown to kill intracellular bacteria, mainly resident in phagocytic cells.[27,28,77–81] However, in nonphagocytic cells, it can be difficult to achieve such an effect in the absence of surface functionalization.[82–86] Therefore, the ability of the bioinspired Eap-functionalized liposomes to facilitate effective intracellular delivery of the poorly permeable anti-infective colistin was investigated. For this purpose, HEp-2 and Caco-2 cells infected with the enteroinvasive bacterium *S. enterica* were employed. After initial optimization of the infection conditions (see Figure S8, Supporting Information), a multiplicity of infection (MOI) of 100 was used to infect cells for 1 h followed by 2 h of gentamicin treatment to kill any extracellular bacteria. Cells containing *S. enterica* were then treated as informed by FACS results for 2 h (HEp-2 cells) or 4 h (Caco-2 cells) with nonfunctionalized or Eap-functionalized (20 μg mL^{-1} Eap) liposomes loaded with 30 μg mL^{-1} colistin. Unloaded liposomes and

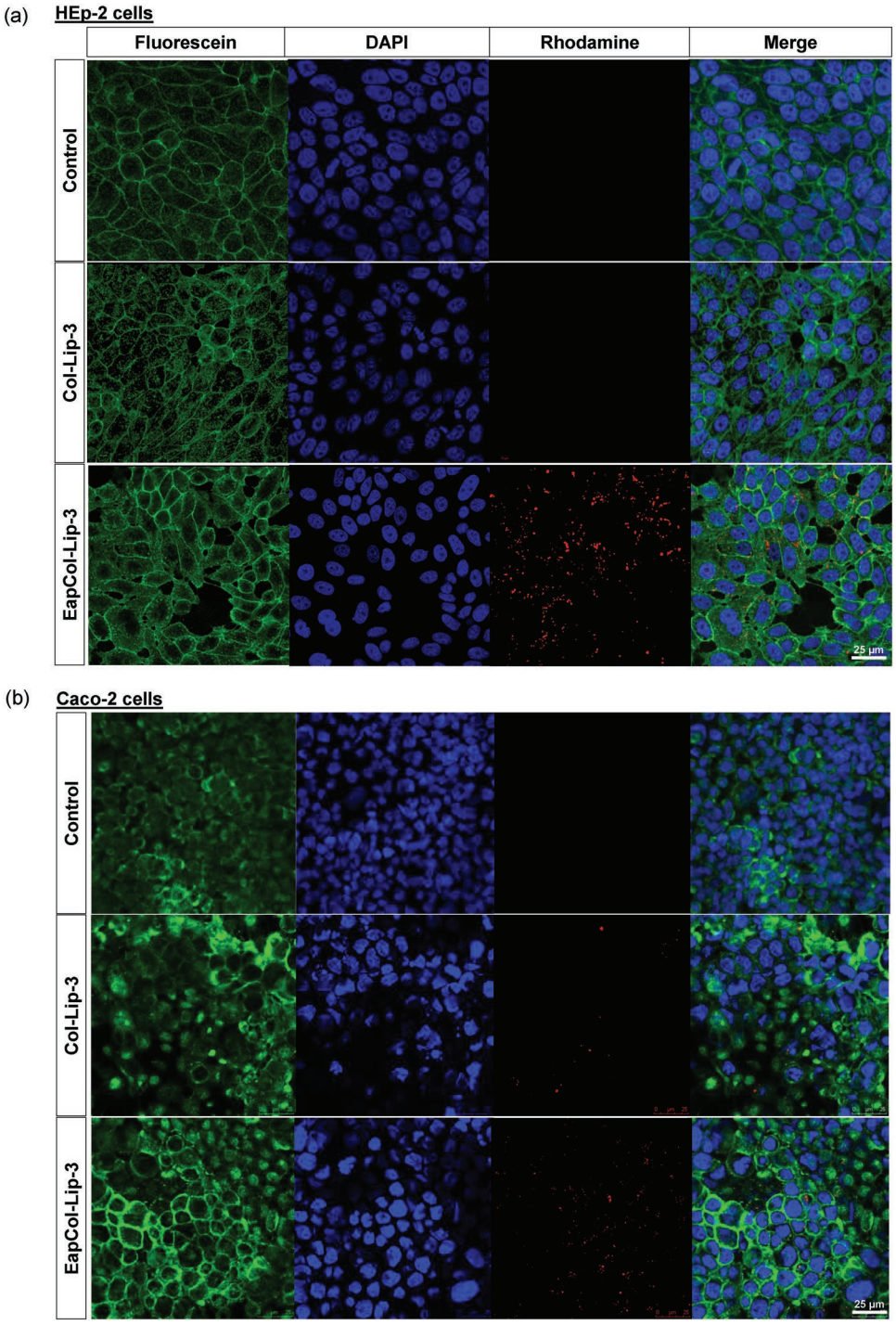

Figure 5. Representative confocal images of a) HEp-2 cells (2 h), b) Caco-2 cells (4 h) of untreated cells (control), treated with non-functionalized colistin liposomes (Col-Lip-3) or Eap-functionalized colistin liposomes (EapCol-Lip-3) are shown. Cell membranes were stained with fluorescein-WGA (green), nuclei were stained with DAPI (blue), and rhodamine-labelled liposomes were visualized as red dotted particles (red).

colistin (as a free drug, 30 µg mL^{-1}) were here utilized as controls. The choice of 30 µg mL^{-1} colistin concentration is based on 10 times the minimum inhibitory concentration (MIC) of colistin acting on *S. enterica* (Figure S9, Supporting Information). Eap concentration was chosen after a dose response study performed with different concentrations of Eap, where the highest bacterial killing percentage was achieved by using 20 µg mL^{-1} Eap in both cell types (Figure S10a,b, Supporting Information). The viability of HEp-2 and Caco-2 cells after infection and liposomal treatment was unchanged in comparison to noninfected/untreated cells (Figure S11, Supporting Information). In both *S. enterica*-infected HEp-2 and Caco-2

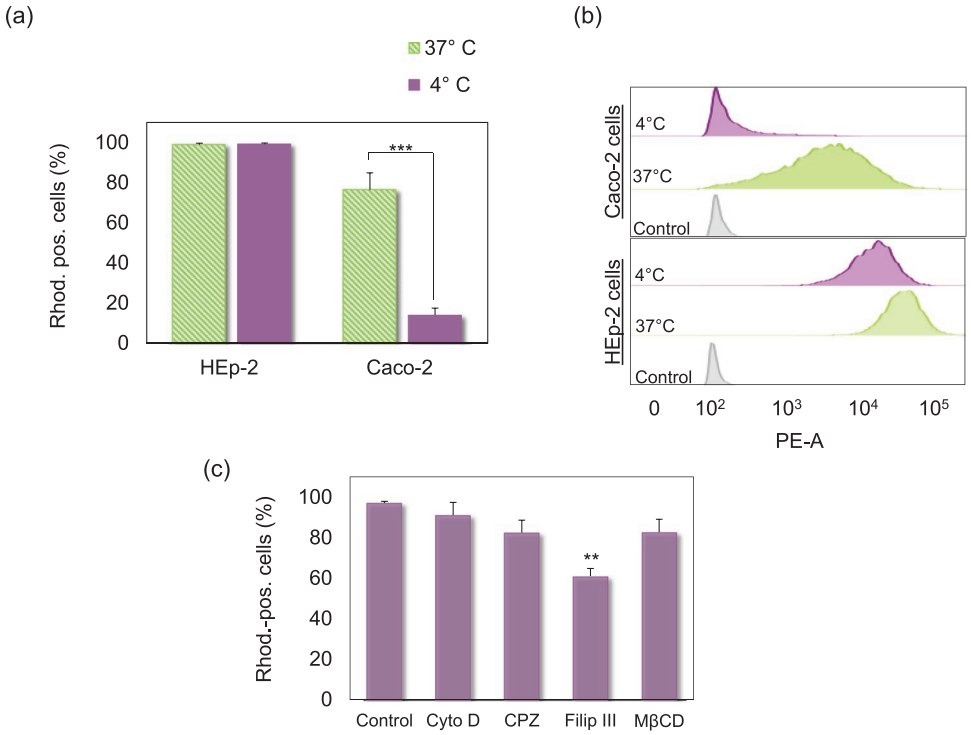

Figure 6. a) Percentages of rhodamine-positive HEp-2 cells and Caco-2 cells and b) the corresponding histogram plots resulting from treatment of cells with colistin-loaded liposomes functionalized with 20 μg mL^{-1} of Eap for 2 h at 37 °C (stripes) and 4 °C (solid). c) Effects of the different endocytosis inhibitors at 37 °C for 1 h; cytochalasin (Cyto D, 1 mg mL^{-1}), chlorpromazine (CPZ, 10 μg mL^{-1}), filipin III (1 μg mL^{-1}), and methyl-β-cyclodextrin/lovastatin (MβCD, 10 mmol L^{-1}/1 μg mL^{-1}), on the internalization of Eap-functionalized liposomes into Caco-2 cells (4 h, 20 μg mL^{-1} Eap was used for functionalization). Control were cells treated with Eap-functionalized liposomes without any inhibitors. Data are shown as mean ± SEM from three independent replicates ($N = 3$, $n = 9$). Significance was defined as $^{**}P < 0.01$ and $^{***}P < 0.001$.

cells, treatment with the Eap-functionalized liposomes loaded with colistin was seen to significantly reduce the intracellular bacterial load by ≈32% and 30% respectively when compared to nonfunctionalized liposomes and free colistin (**Figure 7**). Moreover, treatment of *S. enterica*-infected HEp-2 cells or Caco-2 cells with different concentrations of Eap-functionalized liposomes containing colistin (colistin: 30, 50, 80, 100, 150, and 200 μg mL^{-1}) resulted in a concentration-dependent increase of the bacterial killing to reach a maximum of ≈60% and 40% respectively (Figure S10c,d, Supporting Information). Such a result demonstrates that Eap-functionalized liposomes are not only able to invade into epithelial cells, but also, when drug loaded, are able to release their payload inside cells in order to exert a pharmacological effect. Interestingly, nonfunctionalized

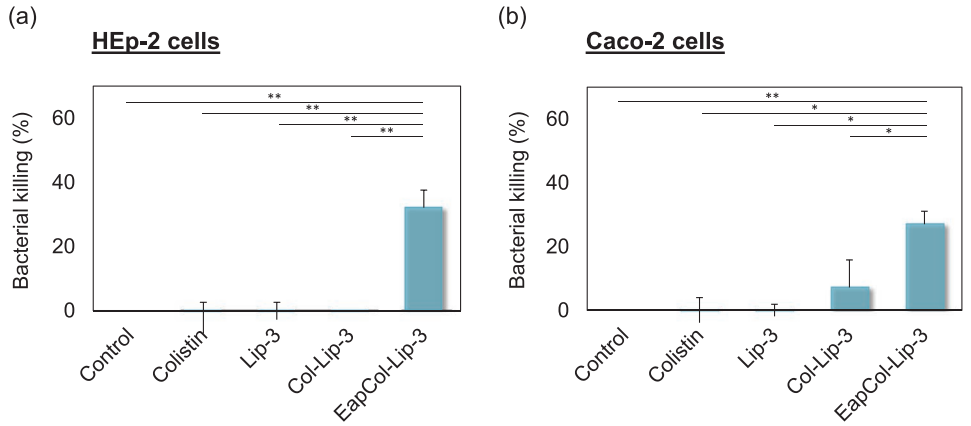

Figure 7. Bacterial Killing percentages of *Salmonella enterica* in a) HEp-2 cells and b) Caco-2 cells after treatment with colistin (Col), empty liposomes (Lip-3), nonfunctionalized colistin liposomes (Col-Lip-3), and Eap-functionalized colistin liposomes (EapCol-Lip-3). In all cases a colistin concentration of 30 μg mL^{-1} was used (Col, Col-Lip-3 and EapCol-Lip-3) and an Eap concentration of 20 μg mL^{-1} was employed, where relevant (EapCol-Lip-3). Data are show as mean ± SEM from four independent replicates ($N = 4$, $n = 12$). Significance was defined as $^{*}P < 0.05$ and $^{**}P < 0.01$.

liposomes loaded with colistin were able to induce only a low degree of bacterial killing in Caco-2 cells, reducing the infection load by 6%. Those liposomes were, although to a lower extent, able to enter cells and release colistin, which is in agreement with uptake results obtained by FACS and confocal laser scanning microscopy (CLSM) (Figures 4 and 5). In a previous study, we could show similar intracellular antibacterial effect with another bacteriomimetic delivery system, namely, InvA497-functionalized liposomes loaded with gentamicin,[29] However, after an oral administration this system is only able to target cells with apically expressed $\alpha_5\beta_1$ integrin receptors, i.e., mainly microfold cells in the small intestine.[87] Eap, on the other hand, is able to interact with different cell types,[88] and, therefore, offers a broader targeting of the gastrointestinal epithelium.

3. Conclusion

A liposomal carrier encapsulating the hydrophilic polypeptide anti-infective, colistin, was first formulated to withstand the acidic and enzymatic environment of the GI tract. This was achieved by combining long chain phospholipids DPPC and DSPC with cholesterol, which increased the stability of liposomes. Subsequently surface functionalization with a bacterial-derived protein, Eap, could be shown to mediate the internalization of these liposomes into epithelial cells. By facilitating intracellularly delivery of their anti-infective cargo, i.e., colistin, which is normally unable to permeate across cellular membranes, a substantial killing of the enteroinvasive bacterium *S. enterica* in epithelial cells was achieved. The Eap-mediated internalization pathway—which has not been well characterized to date—was shown to occur in either an energy dependent or independent manner, varying with cell type. Uptake via an energy-dependent mechanism was in itself determined to involve several different pathways. While this study provides valuable insight into the little-known uptake mechanism of Eap, further investigation is required to dissect the mechanisms by which Eap binds to and is internalized into cells. The current study also showed, for the first time, the potential of Eap as an invasive moiety for intracellular drug delivery. The employed, bioinspired delivery strategy gives a new hope for neglected or problematic antibacterial agents like colistin to be used orally at moderate doses and thereby reducing otherwise prohibitive adverse effects.

4. Experimental Section

Materials: DPPC (Lipoid E PC) and DSPC were kindly provided from Lipoid GmbH (Ludwigshafen, Germany). 1,2-Dipalmitoyl-sn-glycero-3-phospho-ethanolamine-*N*-(lissamine rhodamine B sulfonyl) (ammonium salt) (Rh-DPPE) and DPPE-GA (DPPE-GA) were purchased from Avanti Polar Lipids (Alabama, USA). Colistin sulfate (>90% purity) was obtained from Adipogen GmbH (Hamburg, Germany). Cholesterol and ammonium thiocyanate (NH_4SCN) were purchased from Sigma Aldrich (Steinheim, Germany). Ferric 3-chloride-hexahydrate ($FeCl_3{\cdot}6H_2O$) was obtained from Merck KGaA, Darmstadt, Germany, Biochrom, Germany. All other chemicals and solvents used were at least of analytical grade.

Preparation and Characterization of Colistin-loaded Liposomes: Liposomes were prepared using the lipid film hydration method.[89] Briefly, different liposomal formulations according to Table 1 were prepared by dissolving phospholipids and cholesterol in a mixture of chloroform:methanol (2:1). Rh-DPPE (10 µg mL^{-1}) was additionally added to fluorescently label liposomes. The organic solvents were evaporated using a rotary evaporator (Buchi, Switzerland) with a heating bath heated to 70 °C, at 200 mbar for 1 h. After the formation of a lipid film, different concentrations of colistin solution in phosphate-buffered saline (PBS) were used for hydrating the lipid film (1, 2, 3, 4, 5, and 10 mg mL^{-1}), achieved by continual rotation at 50 °C for 1 h. The resulting vesicles were sonicated for 3 min with a sonication bath and extruded 10 times through 200 nm pore size polycarbonate membranes (Polycarbonate track-Etch Membrane, Sartorius Germany) at 70 °C, using an extruder (LiposoFast L-50, Avestin, Germany). The mean diameter and PDI of liposomes were measured by DLS, while the ζ-potential of liposomes was determined by laser doppler micro-electrophoresis. All physical characterizations were performed using a Zetasizer Nano ZS (Malvern Instruments, United Kingdom).

Liposomes Imaging: SEM and Cryo-TEM were used to visualize liposomal morphologies. For SEM imaging, colistin-loaded liposomes were centrifuged twice at 7000 g for 10 min and pellets were re-suspended in water to remove any traces of PBS. Samples were then diluted 1:20, and a volume of 10 µL was mounted on aluminum stubs, using double-sided adhesive carbon tape and copper grids (Micro to Nano, Netherlands). After drying, samples were sputter-coated with thin gold film using a Quorum Q150R ES sputter-coater (Gala Instrumente GmbH, Germany). SEM imaging was performed using Zeiss EVO HD15 (Zeiss, Germany) under an acceleration voltage of 5 kV, and images were processed with SmartSEM software. Cryo-TEM imaging was conducted by placing a (3 µL) droplet of the liposomes solution onto a S147-4 holey carbon film (Plano, Germany) before blotting to a thin liquid film for 2 s. Afterward samples were plunged at $T = 108$ K into liquid ethane using a Gatan (Pleasonton, USA) CP3 Cryo plunge system and visualized at $T = 100$ K using a JEOL (Akishima, Japan) JEM-2100 LaB6 TEM operating at an accelerating voltage of 200 kV at low-dose conditions.

Entrapment Efficiency and Loading Capacity: Liposomes were purified by centrifugal ultrafiltration using Centrisart tubes fitted with a 300 000 molecular weight cut-off membrane (Sartorius AG, Germany). Centrifugation was carried out at 3270 g and 4 °C for 30 min, and was repeated twice to ensure the complete removal of unencapsulated drug. An HPLC method was then used for quantification of entrapped colistin as previously described with some modifications.[90] Briefly, a Dionex Ultimate 3000 HPLC system (Thermo Scientific, Germany) composed of a pump, a degassing system, an autosampler, a column oven, and a diode array detector was used. A LiChrospher 100 RP-18 (125 × 4 mm, 5 µm) column (Merck KGaA, Germany) was employed. As colistin consists of two components colistin A and B, separation of colistin A and B peaks was achieved using a linear gradient of acetonitrile: (0.1%) trifluoroacetic acid (20:80 to 50:50) over a 10 min period. A flow rate of 1 mL min^{-1} was applied with an injection volume of 100 µL. The oven temperature was set to 30 °C during the analysis. The retention times of colistin A and B were 6.15 and 6.99 min respectively, and the area under the curve (AUC) of both peaks was used for colistin quantification. The entrapment efficiency[91] (EE) and the loading capacity[92] (LC) were calculated according to the following equations

$$\mathrm{EE}(\%) = \frac{\text{quantified amount of colistin}}{\text{initial amount of colistin}} \times 100 \quad (1)$$

$$\mathrm{LC}(\%) = \frac{\text{quantified amount of colistin}}{\text{quantified amounts of phospholipids} + \text{cholesterol} + \text{colistin}} \times 100 \quad (2)$$

Phospholipids amount was determined using a colorimetric assay previously described by Stewart.[93] The assay reagent was prepared by dissolving $FeCl_3{\cdot}6H_2O$ (27.03 g) and NH_4SCN (30.4 g) in water (1 L). Phospholipids standards were prepared in chloroform (0.1 mg mL^{-1}). Liposomes were dissolved in chloroform (1:20) and then an equal volume of the assay reagent was added to the samples and standards. The amount of phospholipids in liposomes was determined by measuring the absorbance at 485 nm. The amount of cholesterol

Table 2. Biorelevant media composition.

Composition	FaSSGF[a)][49]	FaSSIF[b)]/FaSSIF-Enz[c)][50,51]	FeSSIF[d)][52]
Sodium taurocholate [mmol L^{-1}]	0.08	3	15
Phosphatidylcholine [mmol L^{-1}]	0.02	0.75	3.75
Pepsin [mg mL^{-1}]	0.1	–	–
Sodium chloride [mmol L^{-1}]	34.2	105.9	65.1
Oleic acid [mmol L^{-1}]	–	–	5
Monoolein [mmol L^{-1}]	–	–	2.5
Maleic acid [mmol L^{-1}]	–	–	100
Sodium azide [mmol L^{-1}]	–	–	3
Lipase (Pancreatin) [USP mL^{-1}]	–	600[e)]	–
Ad. Deionized water [mL]	1000	500	50
pH	1.6	6.5	6.5

[a)]FaSSGF (Fasted state simulated gastric fluid); [b)]FaSSIF (Fasted state simulated intestinal fluid); [c)]FaSSIF-Enz (Fasted state simulated intestinal fluid containing enzymes); [d)]FeSSIF (Fed state simulated intestinal fluid); [e)]Pancreatin was only added in FaSSIF-Enz.

incorporated in liposomes was quantified using HPLC.[94] The mobile phase consisted of acetonitrile:methanol (70:30 v/v) with a flow rate of 2 mL min^{-1}. Cholesterol peak was detected at a wavelength of 210 nm after 15 min analysis time. Standards were prepared from a stock solution (200 µg mL^{-1}) of cholesterol in (50:50, v/v) acetonitrile:methanol/ethyl acetate (1/1 v/v). Whereas, samples were prepared by dissolving liposomes (400 µL) in acetonitrile:methanol/ethyl acetate mixture (1 mL).

Stability Studies in Biorelevant Media: Stability studies of the prepared liposomes were conducted in fasted state simulated gastric fluid, fasted stated simulated intestinal fluid, and FASSIF containing additional enzymes . Fed state simulated intestinal fluid was also employed. Media were prepared as described in **Table 2**. Liposomes were diluted 1:10 in different media and incubated at 37 °C for 5 h. Samples were collected every hour, purified and analyzed for size, PDI, zeta potential, and colistin content as described above.

Eap Purification: Eap was obtained from *S. aureus* strain Newman[95] as previously described.[96] Briefly, purification of Eap was carried by cation exchange chromatography on a Mono S 5/50 GL column (GE Healthcare, Germany) using a fast-performance liquid chromatography system (Bio-Rad, Germany). Eap-positive fractions were then detected by SDS-PAGE using Coomassie blue staining and pooled to a final concentration of 2 mg mL^{-1}. After sterilization through 200 nm filters (Merck KGaA, Germany), purified Eap was stored at −80 °C until further use.

Liposome Functionalization: Liposomes were functionalized with Eap either covalently (cov) using DMTMM (Sigma Aldrich, Germany) as a coupling reagent or physically via adsorption of Eap to liposomal surfaces (ads). For surface adsorption, liposomes were incubated directly with 40 µg mL^{-1} Eap under stirring (180 rpm) at room temperature for 1 h. For the covalent coupling, carboxylic groups on liposomes were first activated using DMTMM (0.5 mmol L^{-1}) at room temperature under stirring (180 rpm) for 2 h. Afterward, Eap (40 µg mL^{-1}) was added to the surface-activated liposomes under stirring at room temperature for 1 h. The excess of Eap was removed using Centrisart tubes (as described above for purification of unentrapped colistin). The amount of Eap functionalized on liposomes was quantified using SDS-PAGE.[97] Eap standards (5, 10, 20, 30, 40, and 50 µg mL^{-1}), nonfunctionalized liposomes, and Eap-functionalized liposomes were loaded onto the polyacrylamide gel and the electrophoresis was conducted for 40 min at 120 mV. Page Blue Protein staining (Bio-Rad, Germany) was used to stain the gel for 1 h under a gentle shaking. The gel was then rinsed with water and distained in a water bath overnight under a gentle shaking at room temperature. Gel DocTM EZ imager (Bio-Rad, Germany) was used for imaging the gel and ImageJ software to process the images. The functionalization efficiency (FE) was calculated using the following equation[29]

$$FE(\%) = \frac{\text{quantified amount of Eap}}{\text{initial amount of Eap}} \times 100 \quad (3)$$

Cell Culture: Human adenocarcinoma cells of clone HTB-37 (Caco-2) and human laryngeal carcinoma cells (HEp-2) were purchased from American Type Culture Collection (ATCC, Rockville, MD). Caco-2 cells were cultured in 75 cm^2 culture flasks in Dulbecco's Modified Eagle Medium (DMEM, Gibco, Germany) supplemented with 10% fetal calf serum (FCS) (Lonza, Cologne, Germany) and 1% nonessential amino acids (NEAA, Gibco, Germany). HEp-2 cells were cultured in 75 cm^2 culture flasks in Roswell Park Memorial Institute medium (RPMI 1640) (Life Technologies, Paisley, UK) supplemented with 10% FCS. Cells were incubated at 37 °C, 5% CO_2, and 95% relative humidity in an incubator CB 210 (Binder, Germany) and medium was changed every third day. Cells were harvested for experiments using trypsin (0.1%) and EDTA solution (0.02%, Sigma, Steinheim, Germany), and subcultured once a week to maintain the cultures. Cells from passages 30–40 (Caco-2 cells) and 20–32 (HEp-2 cells) were used for all of the experiments.

Uptake Studies: HEp-2 cells were grown on 24-well plates (2×10^4 cells per well) for 72 h, while Caco-2 cells were seeded on Transwell inserts (Corning Incorporated, Acton, MA) with a pore size of 0.4 µm (6×10^4 cells per insert) and allowed to form a differentiated monolayer. Transepithelial electrical resistance (TEER) was measured with an epithelial volt/ohm meter equipped with a Chopstick electrode (World Precision Instruments, USA) over time to monitor the integrity of the Caco-2 cell monolayer, and experiments were performed using monolayers with TEER values ≥500 Ω cm^2. All cells were washed twice with PBS and then incubated with different concentrations (5, 10, 20 µg mL^{-1}) of Eap-functionalized or nonfunctionalized liposomes, or medium (negative control) at 37 °C and 5% CO_2, for 2 or 4 h. Afterward, cells were washed to remove liposomes, harvested, and re-suspended in PBS for flow cytometry analysis (LSRFortessa, BD Bioscience, USA). A minimum of 10 000 live cells were analyzed from forward versus side scatter (FSC versus SSC) gating. The percentage of rhodamine positive cells after taking up Rh-DPPE-containing liposomes was determined with FlowJo 7.6.5 software (FlowJo LLC, USA) using PE channel.

Cell Imaging: HEp-2 cells were seeded at a density of 4×10^4 cells per well on 24-well imaging plates and allowed to grow to 90% confluence. Caco-2 cells were cultivated as a monolayer on glass coverslips (for imaging) and Transwells (for TEER measurements) in 24-well plates and only used for the experiment when TEER values ≥ 500 Ω cm^2 were reached. Cells were treated with liposomes functionalized with Eap (20 µg mL^{-1}), or nonfunctionalized liposomes. Cells were washed with PBS, and then incubated with fluorescein-labeled wheat germ agglutinin (10 µg mL^{-1}) (Vector Laboratories, USA) to stain the cell membrane for 15 min at 37 °C and 5% CO_2. Afterward, cells were washed with PBS and fixed with 3% paraformaldehyde for 30 min at room temperature. Nuclei were stained with 4′,6-Diamidin-2-phenylindol (DAPI, 1 µg mL^{-1}) (Life Technologies, Germany) for 15 min and coverslips were mounted on slides using mounting medium (Thermo, Germany). A confocal laser-scanning microscope (CLSM Leica TCS SP8, Leica Microsystems, Germany) was used to visualize cells. Images were taken with a 25× water immersion objective (1024 × 1024 resolution) and processed using LAS X software (LAS X 1.8.013370, Leica Microsystems, Germany).

Uptake Mechanism: HEp-2 cells were seeded on 24-well plates and Caco-2 cells were seeded on Transwell inserts with TEER values ≥500 Ω cm^2 and incubated with either nonfunctionalized liposomes or Eap-functionalized liposomes at 4 °C for 2 h. Cells were washed with PBS, trypsinized, and then analyzed with flow cytometry. Afterward Caco-2 cells

were subjected to a following experiment using endocytosis inhibitors. Cells grown on Transwells were washed with PBS, then different inhibitors were added separately to both Transwell compartments, chlorpromazine (10 μg mL^{-1}), cytochalasin D (1 mg mL^{-1}), filipin III (1 μg mL^{-1}), and methyl-β-cyclodextrin/ lovastatin (10 mmol L^{-1}/1 μg mL^{-1}) in Hank's Balanced Salt Solution (HBSS).[98,99] After 1 h of incubation at 37° C, liposomes were applied to the apical compartment in the presence of inhibitors and cells were then incubated for another 2 h at 37° C. Afterward, cells were washed, trypsinized, and analyzed with flow cytometry.

Antibacterial Efficacy Assays: Salmonella enterica subsp. *enterica* (Leibniz-Institute DSMZ, Braunschweig, Germany) was cultured in nutrient broth medium (NB) overnight at 37 °C, and then diluted 1:5 in fresh NB and incubated for a further 2.5 h in order to allow bacteria to reach the exponential growth phase. HEp-2/Caco-2 cells were then incubated with *Salmonella* (MOI of 100) at 37 °C, 5% CO_2, and 95% humidity for 1 h, in order to allow for bacterial invasion. Cells were then washed with PBS and incubated with gentamicin solution (50 μg mL^{-1}) for 2 h to kill any extracellular bacteria. Afterward, cells were treated with either Eap-functionalized liposomes (7, 12, 20, or 40 μg mL^{-1} of Eap), nonfunctionalized liposomes containing colistin, or colistin as free drug (colistin dose in all cases = 30 μg mL^{-1}), in order to investigate the impact of Eap concentration on system efficacy; or, with liposomes functionalized with 20 μg mL^{-1} Eap, containing various concentrations of colistin (30, 50, 80, 100, 150, 200 μg mL^{-1}) in order to investigate the occurrence of a colistin dose-response relationship. The final antibacterial assay was performed using liposomes containing 30 μg mL^{-1} colistin and functionalized with 20 μg mL^{-1} Eap. In all cases, formulations were incubated with infected cells for a period of 2 h (HEp-2 cells) or 4 h (Caco-2 cells). Afterward, cells were washed and lysed with ice-cold water. Lysates were plated on nutrient agar plates and incubated at 37 °C for 18 h. Colonies were counted, and the percentage of killing was calculated by normalizing the number of colonies in the treated samples to the ones of untreated control.

Statistical Analysis: All the experiments were performed at least in triplicates and expressed as mean ± SEM. No data preprocessing was performed. One-way-ANOVA followed by a post hoc test was used to calculate statistical significance using OriginPro software (with $*P < 0.05$,$**P < 0.01$, and $***P < 0.001$ considered as significant).

Supporting Information

Supporting Information is available from the Wiley Online Library or from the author.

Acknowledgements

The authors thank Dr. Chiara De Rossi for her support with analytics and confocal imaging, as well as Petra Koenig and Jana Westhues for their support in cell culture. J.E. and M.B. were supported by SFB 1027 grant B2.

Conflict of Interest

The authors declare no conflict of interest.

Keywords

bacterial invasion, bacteriomimetic nanocarriers, Eap, extracellular adherence proteins, simulated intestinal fluids, *Staphylococcus aureus*

Received: May 3, 2019
Revised: June 27, 2019
Published online:

[1] R. K. Ernst, T. Guina, S. I. Miller, *J. Infect. Dis.* **1999**, *179*, S326.
[2] C. D. Britto, V. K. Wong, G. Dougan, A. J. Pollard, *PLOS Neglected Trop. Dis.* **2018**, *12*, e0006779.
[3] A. Karkey, G. Thwaites, S. Baker, *Curr. Opin. Gastroenterol.* **2018**, *34*, 25.
[4] B. A. Golomb, H. J. Koslik, A. J. Redd, *BMJ Case Rep.* **2015**, 2015.
[5] J. Li, R. J. Nation, J. D. Turnidge, R. W. Milne, K. Coulthard, C. R. Rayner, D. L. Paterson, *Lancet Infect. Dis.* **2006**, *6*, 589.
[6] S. Biswas, J.-M. Brunel, J.-C. Dubus, G. M. Reynaudt, J.-M. Rolain, *Expert Rev. Anti-Infect. Ther.* **2012**, *10*, 917.
[7] M. E. Falagas, S. K. Kasiakou, *Clin. Infect. Dis.* **2005**, *40*, 1333.
[8] I. Karaiskos, L. Friberg, K. Pontikis, K. Ioannidis, V. Tsagkari, L. Galani, E. Kostakou, F. Baziaka, C. Paskalis, A. Koutsoukou, H. Giamarellou, *Antimicrob. Agents Chemother.* **2015**, *59*, 7240.
[9] R. L. Nation, S. M. Garonzik, J. Li, V. Thamlikitkul, E. J. Giamarellos-Bourboulis, D. L. Paterson, J. D. Turnidge, A. Forrest, P. F. Silveira, *Clin. Infect. Dis.* **2016**, *62*, 552.
[10] G. G. Rao, N. S. Ly, C. E. Haas, S. Garonzik, A. Forrest, J. B. Bulitta, P. A. Kelchlin, P. N. Holden, R. L. Nation, J. Li, B. T. Tsuji, *Antimicrob. Agents Chemother.* **2014**, *58*, 1381.
[11] F. Shahbazi, *Expert Rev. Clin. Pharmacol.* **2015**, *8*, 423.
[12] R. Singh, J. W. Lillard, *Exp. Mol. Pathol.* **2009**, *86*, 215.
[13] N. Abed, P. Couvreur, *Int. J. Antimicrob. Agents* **2014**, *43*, 485.
[14] H. Pinto-Alphandary, A. Andremont, P. Couvreur, *Int. J. Antimicrob. Agents* **2000**, *13*, 155.
[15] D. Wang, L. Kong, J. Wang, X. He, X. Li, Y. Xiao, *PDA J. Pharm. Sci. Technol.* **2009**, *63*, 159.
[16] J. Li, R. L. Nation, R. W. Milne, J. D. Turnidge, K. Coulthard, *Int. J. Antimicrob. Agents* **2005**, *25*, 11.
[17] E. Sans-Serramitjana, E. Fusté, B. Martínez-Garriga, A. Merlos, M. Pastor, J. L. Pedraz, A. Esquisabel, D. Bachiller, T. Vinuesa, M. Viñas, *J. Cystic Fibrosis* **2016**, *15*, 611.
[18] M. Pastor, M. Moreno-Sastre, A. Esquisabel, E. Sans, M. Viñas, D. Bachiller, V. J. Asensio, A. D. Pozo, E. Gainza, J. L. Pedraz, *Int. J. Pharm.* **2014**, *477*, 485.
[19] Y. Li, C. Tang, E. Zhang, L. Yang, *Pharm. Dev. Technol.* **2017**, *22*, 436.
[20] Z. Drulis-Kawa, A. Dorotkiewicz-Jach, *Int. J. Pharm.* **2010**, *387*, 187.
[21] R. Schiffelers, G. Storm, I. Bakker-Woudenberg, *J. Antimicrob. Chemother.* **2001**, *48*, 333.
[22] W. Wu, Y. Lu, J. Qi, *Ther. Delivery* **2015**, *6*, 1239.
[23] H. He, Y. Lu, J. Qi, Q. Zhu, Z. Chen, W. Wu, *Acta Pharm. Sin. B* **2019**, *9*, 36.
[24] H. T. H. Vu, S. M. Hook, S. D. Siqueira, A. Müllertz, T. Rades, A. McDowell, *Int. J. Pharm.* **2018**, *548*, 82.
[25] M. Daeihamed, S. Dadashzadeh, A. Haeri, M. F. Akhlaghi, *Curr. Drug Delivery* **2017**, *14*, 289.
[26] R. Mout, D. F. Moyano, S. Rana, V. M. Rotello, *Chem. Soc. Rev.* **2012**, *41*, 2539.
[27] M.-H. Xiong, Y.-J. Li, Y. Bao, X.-Z. Yang, B. Hu, J. Wang, *Adv. Mater.* **2012**, *24*, 6175.
[28] F. Gao, L. Xu, B. Yang, F. Fan, L. Yang, *ACS Infect. Dis.* **2019**, *5*, 218.
[29] S. Menina, H. I. Labouta, R. Geyer, T. Krause, S. Gordon, P. Dersch, C.-M. Lehr, *RSC Adv.* **2016**, *6*, 41622.
[30] P. Dersch, R. R. Isberg, *EMBO J.* **1999**, *18*, 1199.
[31] M. Hammel, D. Němeček, J. A. Keightley, G. J. Thomas, B. V. Geisbrecht, *Protein Sci.* **2007**, *16*, 2605.
[32] A. Haggar, M. Hussain, H. Lönnies, M. Herrmann, A. Norrby-Teglund, J. I. Flock, *Infect. Immun.* **2003**, *71*, 2310.
[33] M. Bonazzi, M. Lecuit, P. Cossart, *Cold Spring Harbor Perspect. Biol.* **2009**, *1*, a003087.
[34] M. Flock, J.-I. Flock, *J. Bacteriol.* **2001**, *183*, 3999.
[35] I. Joost, S. Jacob, O. Utermöhlen, U. Schubert, J. M. Patti, M.-F. Ong, J. Gross, C. Justinger, J. H. Renno, K. T. Preissner, M. Bischoff, M. Herrmann, *FEMS Immunol. Med. Microbiol.* **2011**, *62*, 23.

[36] J. Josse, F. Laurent, A. Diot, *F. Microbiol.* **2017**, *8*, 2433.
[37] J. Parmentier, N. Thomas, A. Müllertz, G. Fricker, T. Rades, *Int. J. Pharm.* **2012**, *437*, 253.
[38] T. Róg, *FEBS Lett.* **2001**, *502*, 68.
[39] M.-L. Briuglia, C. Rotella, A. McFarlane, D. A. Lamprou, *Drug Delivery Transl. Res.* **2015**, *5*, 231.
[40] S.-C. Lee, K.-E. Lee, J.-J. Kim, S.-H. Lim, *J. Liposome Res.* **2005**, *15*, 157.
[41] S. J. Wallace, J. Li, R. L. Nation, R. J. Prankerd, B. J. Boyd, *J. Pharm. Sci.* **2012**, *101*, 3347.
[42] Y. F. Mohamed, H. M. Abou-Shleib, A. M. Khalil, N. M. El-Guink, M. A. El-Nakeeb, *Braz. J. Microbiol.* **2016**, *47*, 381.
[43] K. Muppidi, A. S. Pumerantz, J. Wang, G. Betageri, *ISRN Pharm.* **2012**, *2012*, 636743.
[44] J.-P. Colletier, B. Chaize, M. Winterhalter, D. Fournier, *BMC Biotechnol.* **2002**, *2*, 9.
[45] C. Mestresa, M. A. Alsinaa, M. A. Busquetsa, I. Murányib, F. Reigc, *Int. J. Pharm.* **1998**, *160*, 99.
[46] H. Bunjes, T. Unruh, *Adv. Drug Delivery Rev.* **2007**, *59*, 379.
[47] K. J. Fritzsching, J. Kim, G. P. Holland, *Bioch. Biophys. Acta* **2013**, *1828*, 1889.
[48] D. A. Mannock, R. N. A. H. Lewis, R. N. McElhaney, *Biophys. J.* **2006**, *91*, 3327.
[49] M. Vertzoni, J. Dressman, J. Butler, J. Hempenstall, C. Reppas, *Eur. J. Pharm. Biopharm.* **2005**, *60*, 413.
[50] E. Jantratid, N. Janssen, C. Reppas, J. B. Dressman, *Pharm. Res.* **2008**, *25*, 1663.
[51] P. Sassene, K. Kleberg, H. D. Williams, J.-C. Bakala-N'Goma, F. Carrière, M. Calderone, V. Jannin, A. Igonin, A. Partheil, D. Marchaud, E. Jule, J. Vertommen, M. Maio, R. Blundell, H. Benameur, C. J. H. Porter, C. W. Pouton, A. Müllertz, *AAPS J.* **2014**, *16*, 1344.
[52] L. H. Nielsen, S. Gordon, R. Holm, A. Selen, T. Rades, A. Müllertz, *Eur. J. Pharm. Biopharm.* **2013**, *85*, 942.
[53] Y. Y. Lee, A. Erdogan, S. C. S. Rao, *J. Neurogastroenterol. Motil.* **2014**, *20*, 265.
[54] M. Kokkona, P. Kallinteri, D. Fatouros, S. G. Antimisiaris, *Eur. J. Pharm. Sci.* **2000**, *9*, 245.
[55] R. N. Rowland, J. F. Woodley, *Biochim. Biophys. Acta* **1980**, *620*, 400.
[56] B. Lorber, F. Fischer, M. Bailly, H. Roy, D. Kern, *Biochem. Mol. Biol. Educ.* **2012**, *40*, 372.
[57] R. P. Hjelm, C. Schteingart, A. S. Hofmann, D. S. Sivia, *J. Phys. Chem.* **1995**, *99*, 16395.
[58] T. Nawroth, P. Buch, K. Buch, P. Langguth, R. Schweins, *Mol. Pharmaceutics* **2011**, *8*, 2162.
[59] A. Müllertz, C. Reppas, D. Psachoulias, M. Vertzoni, D. G. Fatouros, *J Pharm. Pharmacol.* **2015**, *67*, 486.
[60] D. Riethorst, P. Baatsen, C. Remijn, A. Mitra, J. Tack, J. Brouwers, P. Augustijns, *Mol. Pharmaceutics* **2016**, *13*, 3484.
[61] P. A. Elvang, A. H. Hinna, J. Brouwers, B. Hens, P. Augustijns, M. Brandl, *J. Pharm. Sci.* **2016**, *105*, 2832.
[62] A. J. Clulow, A. Parrow, A. Hawley, J. Khan, A. C. Pham, P. Larsson, C. A. S. Bergström, B. J. Boyd, *J. Phys. Chem. B* **2017**, *121*, 10869.
[63] A. Amici, G. Caracciolo, L. Digiacomo, V. Gambini, C. Marchini, M. Tilio, A. L. Capriotti, V. Colapicchioni, R. Matassa, G. Familiari, S. Palchetti, D. Pozzi, M. Mahmoudi, A. Laganà, *RSC Adv.* **2017**, *7*, 1137.
[64] J. Eisenbeis, M. Saffarzadeh, H. Peisker, P. Jung, N. Thewes, K. T. Preissner, M. Herrmann, V. Molle, B. V. Geisbrecht, K. Jacobs, M. Bischoff, *Front. Cell. Infect. Microbiol.* **2018**, *8*, 235.
[65] I. D. Angelis, L. Turco, *Curr. Protoc. Toxicol.* **2011**, *47*, 20.6.1.
[66] F. Leonard, E.-M. Collnot, C.-M. Lehr, *Mol. Pharmaceutics* **2010**, *7*, 2103.
[67] Y. Kono, H. Jinzai, Y. Kotera, T. Fujita, *Biol. Pharm. Bull.* **2017**, *40*, 2166.
[68] X. Li, D. Chen, C. Le, C. Zhu, Y. Gan, L. Hovgaard, M. Yang, *Int. J. Nanomed.* **2011**, *6*, 3151.
[69] S. Bur, K. T. Preissner, M. Herrmann, M. Bischoff, *J. Invest. Dermatol.* **2013**, *133*, 2004.
[70] S. Gold, P. Monaghan, P. Mertens, T. Jackson, *PLoS One* **2010**, *5*, e11360.
[71] R. Kanlaya, K. Sintiprungrat, S. Chaiyarit, V. Thongboonkerd, *Cell Biochem. Biophys.* **2013**, *67*, 1171.
[72] F. Chen, L. Zhu, Y. Zhang, D. Kumar, G. Cao, X. Hu, Z. Liang, S. Kuang, R. Xue, C. Gong, *Sci. Rep.* **2018**, *8*, 7268.
[73] D. Dutta, J. G. Donaldson, *Cell. Logist.* **2012**, *2*, 203.
[74] S. K. Rodal, G. Skretting, O. Garred, F. Vilhardt, B. van Deurs, K. Sandvig, *Mol. Biol. Cell* **1999**, *10*, 961.
[75] J. Rejman, A. Bragonzi, M. Conese, *Mol. Ther.* **2005**, *12*, 468.
[76] J. E. Schnitzer, P. Oh, E. Pinney, J. Allard, *J. Cell Biol.* **1994**, *127*, 1217.
[77] P. Lutwyche, C. Cordeiro, D. J. Wiseman, M. St-Louis, M. Uh, M. J. Hope, M. S. Webb, B. B. Finlay, *Antimicrob. Agents Chemother.* **1998**, *42*, 2511.
[78] M. Magallanes, J. Dijkstra, J. Fierer, *Antimicrob. Agents Chemother.* **1993**, *37*, 2293.
[79] S. Majumdar, D. Flasher, D. S. Friend, P. Nassos, D. Yajko, W. K. Hadley, N. Duzgunes, *Antimicrob. Agents Chemother.* **1992**, *36*, 2808.
[80] Y. K. Oh, D. E. Nix, R. M. Straubinger, *Antimicrob. Agents Chemother.* **1995**, *39*, 2104.
[81] J. P. Wong, H. Yang, K. L. Blasetti, C. J. G. Schnell, J. Conley, L. N. Schofield, *J. Controlled Release* **2003**, *92*, 265.
[82] N. A. Atchison, W. Fan, K. K. Papas, B. J. Hering, M. Tsapatsis, E. Kokkoli, *Langmuir* **2010**, *26*, 14081.
[83] M. B. Hansen, E. van Gaal, I. Minten, G. Storm, J. C. M. van Hest, D. W. P. Löwik, *J. Controlled Release* **2012**, *164*, 87.
[84] H. I. Labouta, S. Menina, A. Kochut, S. Gordon, R. Geyer, P. Dersch, C. M. Lehr, *J. Controlled Release* **2015**, *220*, 414.
[85] W. Fan, D. Xia, Q. Zhu, L. Hu, Y. Gan, *Drug Discovery Today* **2016**, *21*, 856.
[86] A. Goes, G. Fuhrmann, *ACS Infect. Dis.* **2018**, *4*, 881.
[87] M. A. Clark, B. H. Hirst, M. A. Jepson, *Infect. Immun.* **1998**, *66*, 1237.
[88] N. Harraghy, M. Hussain, A. Haggar, T. Chavakis, B. Sinha, M. Herrmann, J.-I. Flock, *Microbiology* **2003**, *149*, 2701.
[89] A. D. Bangham, M. M. Standish, J. C. Watkins, *J. Mol. Biol.* **1965**, *13*, 238.
[90] L. Bai, Z. Ma, G. Yang, J. Yang, J. Cheng, *J. Chromatogr. Sep. Tech.* **2011**, *2*, 1000105.
[91] Z. Zhang, S. S. Feng, *Biomaterials* **2006**, *27*, 4025.
[92] S. Papadimitriou, *J. Controlled Release* **2009**, *138*, 177.
[93] J. C. Stewart, *Anal. Biochem.* **1980**, *104*, 10.
[94] N. Simonzadeh, *J. Chromatogr. Sci.* **2009**, *47*, 304.
[95] E. S. Duthie, L. L. Lorenz, *J. Gen. Microbiol.* **1952**, *6*, 95.
[96] A. N. Athanasopoulos, M. Economopoulou, V. V. Orlova, A. Sobke, D. Schneider, H. Weber, H. G. Augustin, S. A. Eming, U. Schubert, T. Linn, P. P. Nawroth, M. Hussain, H.-P. Hammes, M. Herrmann, K. T. Preissner, T. Chavakis, *Blood* **2006**, *107*, 2720.
[97] A. B. Nowakowski, W. J. Wobig, D. H. Petering, *Metallomics* **2014**, *6*, 1068.
[98] L. M. Alexander, S. Pernagallo, A. Livigni, R. M. Sánchez-Martín, J. M. Brickman, M. Bradley, *Mol. BioSyst.* **2010**, *6*, 399.
[99] J. Zhang, X. Zhu, Y. Jin, W. Shan, Y. Huang, *Mol. Pharmaceutics* **2014**, *11*, 1520.